World Conference on Timber Engineering Oslo 2023

EXPERIMENTAL MONOTONIC AND CYCLIC TESTING ON GLULAM BEAM-TO-COLUMN CONNECTIONS

Erica C. Fischer[1], Haley Madland[2], Sujit Bhandari[3], Arijit Sinha[4]

ABSTRACT: During seismic events, mass timber gravity connections must be able to accommodate the induced lateral deformations while still maintaining their load bearing capacity. Large-scale experimental testing can demonstrate and provide data for different connection configurations and numerical simulations can further inform the behaviour of these connections under lateral demands. However, there is a lack of experimental testing on glue laminated (glulam) beam-to-column connections, which presents a lack of data available for benchmarking numerical modelling. This paper will summarize a comprehensive large-scale testing regime performed at Oregon State University on five glulam beam-to-column connections, three custom designed connections and two pre-engineered connections. Each connection was tested under both monotonic and cyclic loading demands and the data from one of the connection tests was used to develop preliminary numerical modelling techniques for glulam beam-to-column connections. The tests demonstrated that all of the connections were able to be tested to 7.2% drift in the monotonic test and 4% drift in the cyclic test without losing load bearing capacity. The experimental testing regime developed data on maximum force demands in the connections, connection rotations, and connection stiffnesses that were used to characterize the connections on a scale of pinned to fixed connections.

KEYWORDS: Mass timber, Beam-to-column connection, Deformation compatibility, Monotonic, Cyclic

1 INTRODUCTION

Gravity beam-to-column connections in a building are designed to transfer shear forces, to be capable of rotation, and to have some small resistance to lateral forces. During a seismic event, where lateral forces are applied to a building, the entire building will also be subjected to deformation demands. Because of this, every member in the structure, including the gravity connections, must be capable of deforming along with the rest of the structure. Loss of load carrying capacity of gravity connections can occur when the connection components do not have sufficient ductility or strength to deform with the remainder of the building under lateral demands. This could potentially have cascading effects leading to a partial or complete collapse of the structure itself. Therefore, it is extremely important that the ductile behaviour of gravity connections under lateral loading is understood and promoted in design. This behaviour is referred to as deformation compatibility.

To better understand the deformation compatibility behaviour of beam-to-column connections, they are tested under monotonic and cyclic lateral loading. The experimental data from these tests informs connection characteristics such as the force-deformation (F-δ) and moment-rotation (M-θ) relationships of the connection. However, there is minimal research on deformation compatibility behaviour glulam beam-to-column connections. Because of this, the deformation compatibility behaviour of glulam beam-to-column connections is not well understood.

Glulam beam-to-column connections typically fall into one of two categories: custom designed connections or pre-engineered connections. For custom design connections, the responsibility of designing the connection is placed on the engineer of record. However, pre-engineered connections are proprietary connections that have been designed, tested, and rated for certain loading by a supplier. This means that once the required capacity of a connection has been determined by the engineer, a pre-engineered connection can be selected using design aids developed by the supplier of the connection. Therefore, while custom connections can be specifically designed to meet the necessary capacity requirements most efficiently, more time spent designing is required of the engineer. Conversely, pre-engineered connections can reduce the design time for the engineer,

[1] Assistant Professor, Oregon State University, School of Civil and Construction Engineering, Corvallis, OR, erica.fischer@oregonstate.edu
[2] Graduate Research Assistant, Oregon State University, School of Civil and Construction Engineering, Corvallis, OR< madlanha@oregonstate.edu
[3] Post-doctoral researcher, Oregon State University, School of Civil and Construction Engineering, Corvallis, OR, sujit.bhandari@oregonstate.edu
[4] Arijit Sinha, Associate Professor, Oregon State University Dept. of Wood Science & Engineering, Corvallis OR, arijit.sinha@oregonstate.edu

https://doi.org/10.52202/069179-0290

but limited options may force the engineer to use an over-designed connection.

The design of custom glulam beam-to-column connections is prescribed by relevant standards, such as ASCE 7-16 [1] and the National Design Specification for Wood [2]. The required lateral capacity of a gravity connection is defined in Section 1.4 of ASCE 7-16 as no less than 5% of the supported members weight, and no less than 5% of the reaction imposed on the supporting member due to the unfactored dead and live loads [1]. Although gravity connections are not intended to resist large lateral forces, these integrity provisions in Section 1.4 ensure that there is some connection between members capable of withstanding a minimum prescribed lateral force. However, although custom connections are designed for this lateral force there is no correlation between this lateral force demand and the deformations or rotations of the connection. Therefore, the behaviour of connections exposed to large deformations is not addressed.

To demonstrate the capacity of pre-engineered connections and provide design aids to the engineer for choosing pre-engineered connections, suppliers must perform experimental testing [3] to establish allowable loads in the connection. This testing prescribes how connection characteristics such as the limiting strength and deflection should be determined but does not address the deformation compatibility behaviour of the connection. Testing such as this creates substantial barriers to the development of pre-engineered connections because of the large time and financial investments that must be spent to perform experimental testing.

The research presented and discussed in this paper serves to develop a fundamental understanding of the behaviour of glulam beam-to-column connections exposed to lateral monotonic and cyclic loading. Monotonic and quasi-static cyclic testing of both custom and pre-engineered glulam beam-to-column connections involving combined lateral and gravity loading were performed, from which quantitative data was collected and qualitative observations were made. From the experimentally collected data, the force-displacement (F-δ) and the moment-rotation (M-θ) relationships were compared between connections. Connection characteristics such as initial and secant stiffness and energy dissipation were calculated and compared across custom and pre-engineered connections. The data developed from the experimental testing regime was used to develop and benchmark a finite element method model and explore numerical modelling methods for glulam beam-to-column connections. Specifically, the objectives of this research are to: (1) quantify the deformation compatibility behaviour of glulam beam-to-column connections under lateral loading demands, (2) compare the deformation compatibility behaviour of custom and pre-engineered beam-to-column connections, and (3) explore numerical modelling methodologies for simulating glulam beam-to-column connections under lateral demands.

2 MATERIALS AND METHODS

2.1 TESTING SETUP

The testing setup (Figure 1) consisted of a 3.66 meter tall 24F-V4 glulam Douglas Fir (DF) column, connected at its base to a pin connection. The beam, a 24F-V4 DF glulam, extended approximately 4.27 meters from the face of the column, at mid-height in all connection types. The beam was 311 mm (W) x 610 mm (D). The column width was 311 mm in all connections, but depth varied on connection type. The end of the beam was supported by a roller support. A 1.2 meter wide, 4.27 meter long, and 175 mm thick SPF CLT (5-ply) deck was connected to the top of the beam. A hydraulic ram applied a constant gravity load throughout the tests.

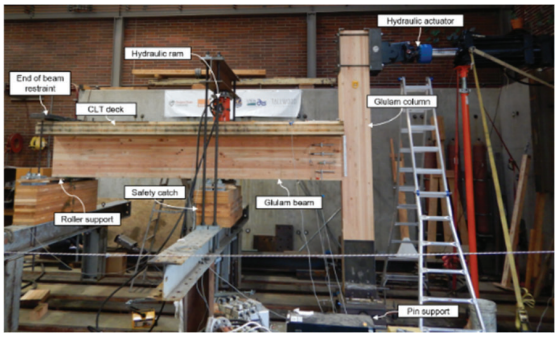

Figure 1: *Testing setup*

2.2 SPECIMEN DESCRIPTIONS

Five connections were investigated. Three connections were designed at Oregon State University per relevant standards [1, 2] and two connections were pre-engineered connections, designed by MTC Solutions. Specimen designations include the connection number, a shortened descriptor of the connection, and loading type (M for monotonic and Cyc for cyclic). For example, C1-KP-Cyc1 refers to connection 1 (C1), the connection uses a knife plate (KP), and the first cyclic test performed (Cyc1) on that connection type. For brevity the connections are referred to only by their designation. Connection C1-KP was a bracketed knife plate connection (Figure 2a). Connections C2-N and C3-N2 were bearing connections where the beam was inserted into a notched column (Figures 2b and 2c). Connection C4-MEG was a MEGANT 450x150x50 concealed beam hanger (Figure 2d), and connection C5-MTCP was a prototype connection designed by MTC (Figure 2e). Both MTC connections involved two interlocking aluminium plates, one screwed to the beam, and one to the column. A more comprehensive description of the connections is provided in [4, 5].

https://doi.org/10.52202/069179-0290

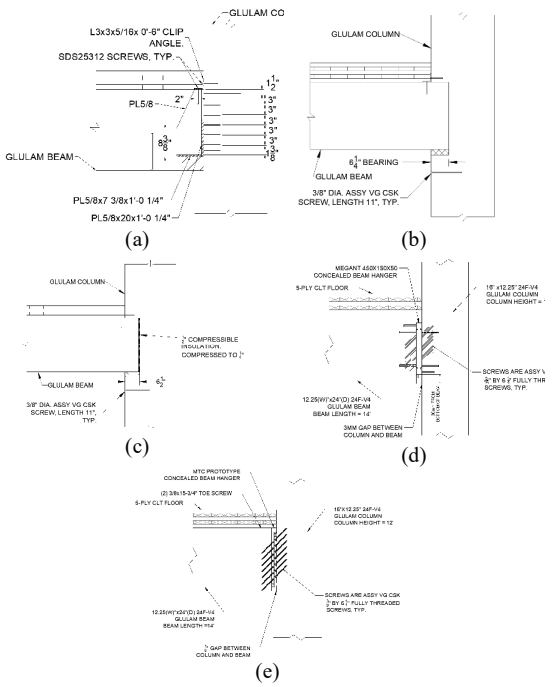

Figure 2: *Glulam beam-to-column connections*

2.3 LOADING PROTOCOL

For monotonic tests, displacement was applied through a hydraulic actuator at a rate of 0.51 mm/second to a target drift of 7.2%. The abbreviated CUREE basic loading history [6] with a target reference deformation of 1.9% drift and maximum displacement of 3.8% drift was used for the cyclic tests (Figure 3). The cyclic test began at a rate of 0.25 mm/second and increased to 0.64 mm/second after the cycle with the reference deformation. The cyclic loading protocol was altered for connections C4-MEG-Cyc2, C5-MTCP-Cyc1, and C5-MTCP-Cyc2, such that the cycle of maximum displacement was increased to 4% drift (from 3.8%), and the following trailing cycle was increased to 75% of the 4% drift cycle.

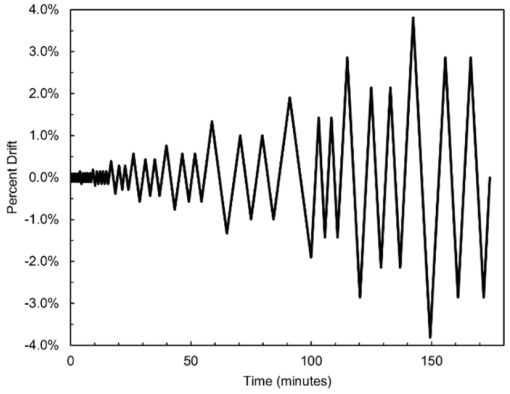

Figure 3: *Cyclic loading protocol per CUREE [6]*

The design shear demands for connections C1-KP, C2-N, and C3-N2 were calculated using an archetype office building with glulam beams spaced at 3.66 m, columns spaced at 8.53 m, and a live load of 2.39 kPa [1]. The design lateral demand were calculated per Section 1.4 of ASCE 7-16 [1]. To resist this lateral demand, and to have a mechanical connection between the glulam beam and column, each of these connections used an L3x3x5/16x152 mm section connected to the beam and column with two SDS25312 screws each. To install this clip angle on the top of the beam, a small portion of the CLT was chipped out to not conflict with the clip angle. The design shear demands for connections C4-MEG-M and C5-MTCP-M were prescribed by the supplier, MTC Solutions. Additional information on these demands can be found in [4, 5]. A summary of these demands and capacities is shown in Table 1.

Table 1: *Summary of gravity and lateral loading demands on connections*

Connection designation	Design shear demand [kN]	Design lateral capacity (demand) [kN]
C1-KP	49.1	6.09 (2.4)
C2-N	49.3	
C3-N2	49.3	
C4-MEG	98	14.5
C5-MTCP	179	17.3

2.4 INSTRUMENTATION LAYOUT

For both the monotonic and cyclic testing, seven linear variable differential transformers (LVDTs) and three load cells were utilized to measure the displacement and calculate the behaviour of the connections (Figure 4). In addition, the hydraulic actuator head displacement and a string potentiometer were utilized to measure the movement of the column. These measurements were used to calculate story drift throughout the test. LVDTs #1 – 4 were utilized to calculate the rotation of the connection assuming rigid body rotation of the column. These connection rotations were then compared with the base connection rotations calculated using LVDTs #5 and #6 to confirm the assumption of rigid body rotation. LVDTs #5 and #6 measured vertical displacements throughout the duration of the test and were centred on the column such that the recorded data could be used in combination with the known distance between the two LVDTs to calculate the column base rotation. Lastly, LVDT #7 was used to measure the differential movement between the top of the CLT and the column itself.

The load cells under the beam end, the ram, and the column base were utilized to calculate the shear in the connection throughout the test (Table 1). Connection moment was calculated throughout the test by multiplying the measured actuator force by the distance between the actuator force and the mid-height of the beam.

https://doi.org/10.52202/069179-0290

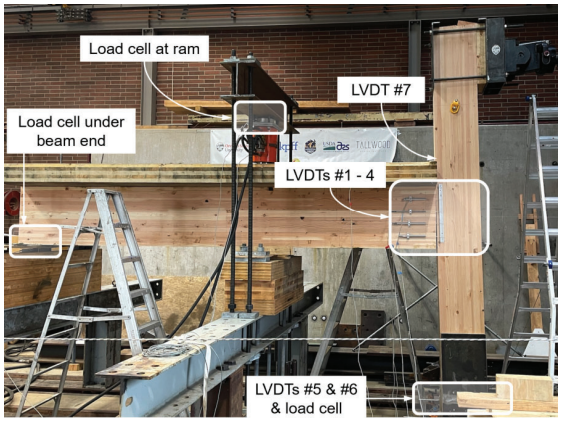

Figure 4: *Instrumentation layout for connection tests*

2.5 NUMERICAL MODELING METHODOLOGY

A three-dimensional finite element method (FEM) model of C2-N-M was developed in the commercially available software, Abaqus CAE, to explore the methodology for simulating glulam beam-to-column connections and to further understand the experimental test. The dimensions of the glulam beam, column, and CLT deck matched those tested in the laboratory at Oregon State University. An additional part was added to the base of the column such that the point of rotation for the column base matched that experimentally tested. Steel material properties were applied to this part to limit deformations. In addition, rather than applying boundary conditions to the beam end directly, an end of beam support was simulated to explore if friction contributed to the stiffness of the connection. Deformations were applied through a displacement-controlled loading protocol at the same rate as described in Section 2.3 at where the centroid of the actuator was located. The FEM model is shown in Figure 5.

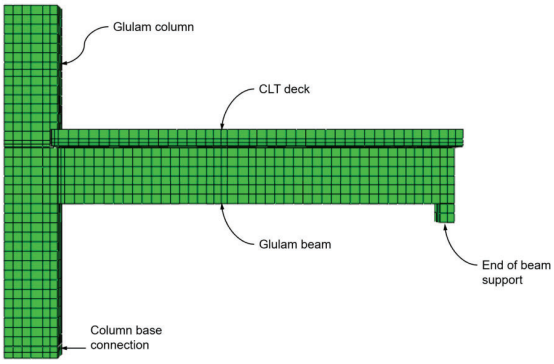

Figure 5: *FEM model of C2-N-M*

The column base was restrained from rotation in the out-of-plane direction and movement in all directions, but allowed to rotate about the base. The beam end was restrained from vertical displacement and rotation but was allowed to move horizontally.

As an anisotropic material, wood's stiffness and strength properties vary in different directions. Usually, the property of wood is defined in three directions: longitudinal (L), radial (R), and tangential (T). The strength and stiffness properties are typically higher in the longitudinal direction compared to radial and tangential directions. The stress-strain relationship for wood is typically linear until brittle failure for tension and shear loading in all directions while the stress-strain relationship is typically nonlinear and ductile in compression. For the FEM model described within this paper, wood has been modelled as orthotropic material with elastic-perfectly plastic behaviour [7, 8]. The stiffness properties for 24F-V4 DF glulam are from NDS and Wood Handbook [2] while the properties for SPF E1 CLT are taken from PRG 320 [9].

The coefficient of friction between the glulam column and beam was assumed to be 0.5 and the coefficient of friction between the glulam beam end and end support was varied to explore the degree of "frictionless" the authors were able to attain.

3 EXPERIMENTAL RESULTS

3.1 MONOTONIC TESTING

The yield load, yield displacement, and initial stiffness were calculated per EN12512 [10] and are summarized in Table 2. Specimen C2-N-M was the only specimen to have post-peak behaviour during monotonic testing. The remainder of the specimens reached maximum load (F_{max}) at maximum displacement.

Specimens C1-KP-M and C2-N-M had the lowest of the F_{max} with F_{max} increasing by 260% between C2-N and C3-N2 connections. The addition of the compressible insulation increased the capacity of the connection. The pre-engineered connections had larger F_{max} than the custom connections, even with the application of larger shear demands throughout the test.

Table 2: *Calculated properties for connections under monotonic loading*

Connection designation	Max. load [kN]	Yield load [kN]	Yield displ. [mm]	Initial stiffness [N/mm]
C1-KP	8.72	4.84	10.9	446
C2-N	11.97	8.87	15	595
C3-N2	21.42	18.46	28.4	649
C4-MEG	29.17	15.82	33.8	467
C5-MTCP	36.48	25.16	27.7	913

A small yield displacement (d_y) can indicate less ductility within the connection whereas a larger d_y, particularly coupled with a larger yield force (F_y) can indicate more ductility within the connection. In addition, higher values of initial stiffness can potentially indicate that the connection has more rotational rigidity. This type of behaviour is more evident in the initial stiffness

https://doi.org/10.52202/069179-0290

calculations where C4-MEG connection has lower initial stiffness than some of the custom connections (C2-N and C3-N2). C5-MTCP-M had the largest initial stiffness, 105% greater than the initial stiffness of specimen C1-KP-M. Connections C3-N2-M, C4-MEG-M, and C5-MTCP-M all had considerably larger d_y values than C1-KP-M and C2-N-M, ranging between 28 – 34 mm.

The design-level drift demand for buildings is 2% drift [1]. The actuator force at a lateral displacement corresponding to 2% drift for each test was compared to the design lateral capacity for each connection. For every connection, the actuator force exceeded the design lateral capacity at a drift of 2%. Table 3 summarizes the ratio of the actuator force at 2% drift ($P_{2\%}$) to the design lateral capacity of connection (P_n). However, failure of the connections (loss of load carrying capacity) was not observed during any of the tests. Therefore, although the lateral capacity of the connection was exceeded, force transfer continued through the connection for the duration of the tests.

Table 3: *Ratio of actuator force at 2% drift to design lateral capacity of tested connections*

Connection designation	$\frac{P_{2\%}}{P_n}$
C1-KP	1.13
C2-N	1.56
C3-N2	3.54
C4-MEG	1.22
C5-MTCP	1.79

During monotonic testing of the connections, screw fracture occurred in the C4-MEG connection, and fracture of the column connection plate occurred in the C5-MTCP connection. In the C2-N and C3-N2 connections, withdrawal of the screws connecting the clip angle to the column was observed.

3.2 CYCLIC TESTING

Backbone curves of all cyclically tested specimens, constructed from the peak actuator force and corresponding story drift in each primary cycle, are plotted in Figure 6. Connections C2-N and C3-N2 had similar forces during pulling cycles, but C3-N2 connections had substantially larger forces during pushing cycles, indicating greater capacity. Overall, custom connections generally had lower actuator forces than pre-engineered connections.

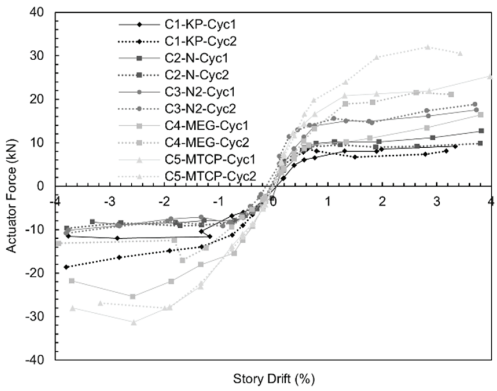

Figure 6: *Backbone curves of cyclic tests*

In Figure 7, the connection moment-rotation relationship is plotted for all cyclically tested specimens, with backbone curves (shown in black) constructed from peak connection moments and corresponding rotations in each primary cycle. The same trends were also observed for actuator forces due to the nature of how connection moments were calculated. As such, pre-engineered connections generally demonstrated larger connection moments than custom connections. The large drop in moment during the pushing cycle of the largest amplitude primary cycle for C5-MTCP-Cyc2 corresponds to the fracture of the column connection plate pocket (Figure 7).

The secant stiffness for each primary cycle was calculated for each connection, similar to previous research [11, 12], and plotted against connection rotation. These plots (Figure 8) show the calculated secant stiffness of the specimens decreases throughout the test. The secant stiffness is the ratio of the summation of the absolute value of the maximum ($+M_i$) and the minimum ($-M_i$) connection moment attained during a primary cycle to the summation of the absolute value of the rotation that corresponds to $+M_i$ ($+\Delta_i$) and the absolute value of the rotation that corresponds to $-M_i$, ($-\Delta_i$). The secant stiffness degraded with increasing connection rotation for each specimen. The secant stiffness decreased 74 – 91% from the first to the last primary cycle. The decrease of secant stiffness can indicate damage accumulating in a connection. While damage is expected, rapid decreases in secant stiffness indicate more brittle behaviour while gently decreasing slopes indicate more ductile behaviour. Although lateral force demands on connections are lower in early primary cycles, it is in these early loading cycles that the greatest stiffness degradation occurred. Greater secant stiffness indicated greater rotational rigidity in the connection as a larger force, or moment, is required to achieve the same connection rotation.

https://doi.org/10.52202/069179-0290

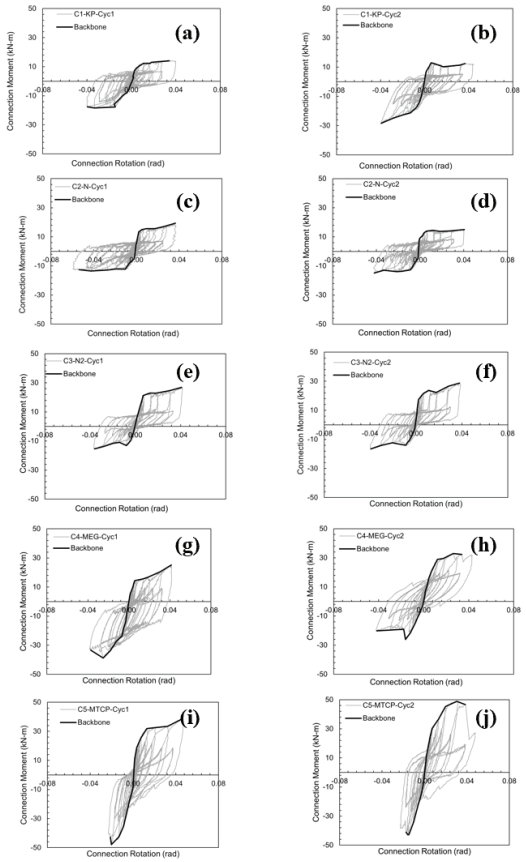

Figure 7: *Connection moment rotation relationship for cyclic tests (a) C1-KP-Cyc1, (b) C1-KP-Cyc2, (c) C2-N-Cyc1, (d) C2-N-Cyc2, (e) C3-N2-Cyc1, (f) C3-N2-Cyc2, (g) C4-MEG-Cyc1, (h) C4-MEG-Cyc2, (i) C5-MTCP-Cyc1, (j) C5-MTCP-Cyc2*

An increase in secant stiffness was observed between the first (0.075∆) and second primary cycles (0.1∆) except for C1-KP-Cyc2, C3-N2-Cyc1, C4-MEG-Cyc1, and C4-MEG-Cyc2. After the 0.1∆ primary cycle, as damage accumulated, specimens demonstrated a non-linear decrease in secant stiffness from one consecutive primary cycle to the next. The largest rate of decreasing secant stiffness occurred between the 0.1∆ and 0.2∆ primary cycles except for connections C1-KP and C4-MEG. These specimens had the largest rate of decreasing secant stiffness either between primary cycles 0.075∆ and 0.1∆ (C1-KP-Cyc2, C4-MEG-Cyc1, and C4-MEG-Cyc2), or primary cycles 0.2∆ and 0.3∆ (C1-KP-Cyc1). Both C2-N specimens exhibited the largest percent degradation of secant stiffness from the first to the last primary cycle (91% in each case). Pre-engineered connections had the largest secant stiffnesses, displaying more rigidity than custom connections. However, C4-MEG specimens had lower rates of decreasing secant stiffness than the C5-MTCP specimens, indicating more ductile behaviour.

To compare the per-cycle energy dissipated, equivalent viscous damping ratio (EVDR) was used. This ratio is the energy enclosed in the moment-rotation hysteretic loop (Figure 7) divided by the corresponding energy that a linear system undergoing the same maximum rotation and corresponding moment would have dissipated. This ratio is then divided by 2π. A higher EVDR indicates that the connection has better energy dissipation. Between the 0.075Δ and 0.1Δ primary cycles, specimens C2-N-Cyc1, C2-N-Cyc2, and C5-MTCP-Cyc1 had large increases (between 54-203%) in EVDR while all other connections tested exhibited either much smaller increases or even decreases in EVDR. These sharp increases indicate damage occurring within the connection due to energy being dissipated. All of the C2-N and C3-N2 connections tested exhibited a small peak in EVDR during the 0.7Δ primary cycle (1.33% drift). During these cycles, the authors observed screw withdrawal of C2-N-Cyc1, and deformation of the clip angle during testing of C2-N-Cyc2. The EVDR of the custom connections either plateaued or decreased between the final primary cycles (1.5Δ to 2.0Δ); however, the EVDR of the pre-engineered connections increased with increasing connection rotation. This behaviour indicates that pre-engineered connections exhibited improved energy dissipation compared to custom connections, with larger total energy dissipation, and increasing EVDR values throughout testing.

4 NUMERICAL MODELING RESULTS

The authors compared the results from the FEM model with the experimental data for only C2-N-M testing to explore modelling methodologies for glulam beam-to-column connections. The authors found that the numerical model and the experimental data had good agreement for drift levels less than 1.4% drift (Figure 8). The comparison of energy differential between the experimental data and the FEM model was less than 20% and reduced substantially throughout testing. The results shown in Figure 8 used a coefficient of friction of 0.1 between the beam end and beam end support. The difference in the experimental data and the numerical modelling resides in the material model. While the behaviour of the FEM model and experimental data at maximum drift look similar (Figure 9), there is crushing of the glulam beam at the top of the connection pocket. The nature of the material model that was utilized within the FEM model described in this paper did not implement simulating crushing of the glulam.

https://doi.org/10.52202/069179-0290

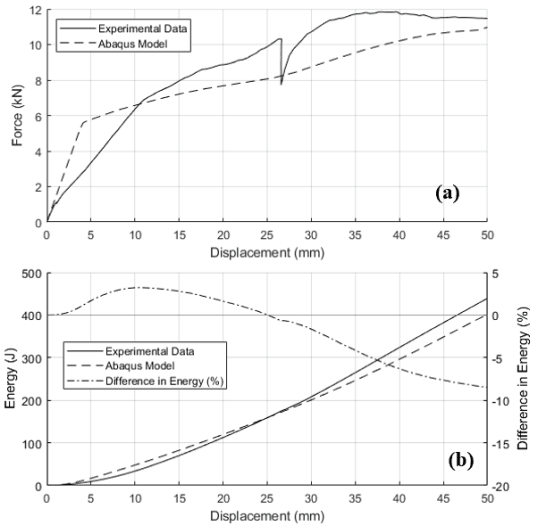

Figure 8: *Comparison of experimental test data to FEM model (a) force-displacement comparison and (b) quantifying energy differences between experimental data and FEM model*

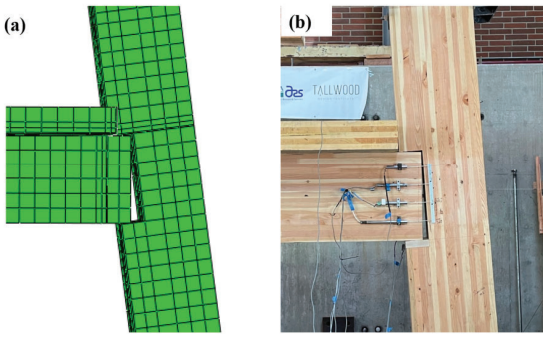

Figure 9: *Comparison of FEM model connection behaviour and experimental test at maximum drift (7.2%)*

Previous researchers have tried to implement damage and crushing material models into FEM simulations to simulate crushing of timber. However, many of these simulation techniques requires the researcher to know where localized crushing will occur prior to the simulation and therefore are limited for predictive modelling of untested connections. Hill yield criterion, sometimes with modifications, has been used to simulate the post-peak behaviour of wood for modelling of timber connections [13 -16]. To simulate the crushing around the steel members in connections, a so-called "foundation" modelling approach based on the theory of a beam on a nonlinear foundation has been used [15, 17, 18]. In these simulations, a material model with lower strength and stiffness was applied where localized crushing was expected. Crushable foam material model has also been used to simulate the crushing of wood in numerical models [19]. While this model simulated crushing at the bearing surfaces and the numerical model provided comparable results to the experiment, this isotropic material model doesn't consider the orthotropic behaviour of wood.

User subroutines incorporating different behaviour of wood have also been used in numerical modelling. Modified Hashin-Hill yield criterion implemented in a user subroutine has been used to model a bolted glulam beam-to-column connection. The model was able to simulate the cracking of wood similar to that seen in the experiment [13]. A more sophisticated constitutive model combining a number of sub-models, including orthotropic elasticity, Yamada-Sun failure criteria, softening, and hardening, was incorporated into a user subroutine for Abaqus [20]. The behaviour of wood in compression was modelled using strain-based damage evolution, plastic-flow, and hardening law. This model was able to reasonably simulate the mechanical as well as thermal behaviour of wood in bending and connections; however, creates a large burden on the researcher to write the subroutine and validate the subroutine against experimental data prior to predictive modelling.

5 CONCLUSIONS

Seismic events can create both force and deformation demands on a building. Beam-to-column connections must be capable of deforming with the rest of the structure during these events while maintaining load-carrying capacity. This behaviour is referred to as deformation compatibility and can be quantified through experimental testing. Because of the novelty of mass timber as a structural material, very limited experimental data has been produced on the deformation compatibility behaviour of glulam beam-to-column connections, therefore this behaviour is not yet well understood. To meet this demand of experimental data, five different connection designs were investigated. Three were custom connections (C1-KP, C2-N, and C3-N2), and two were pre-engineered connections (C4-MEG and C5-MTCP).

Large scale monotonic tests were performed on connections to a target deformation of 7.2% drift. Larger lateral forces were present in connection C3-N2 than C2-N, indicating the addition of compressible insulation increased capacity in the connection. Connection C5-MTCP had the largest initial stiffness and secant stiffness, while C4-MEG had the had the second lowest initial stiffness, and the largest yield displacement, indicating more ductile behaviour.

In cyclic tests, the cycle of maximum displacement corresponded to a target story drift between 3.81 - 4.0%. The hysteretic force-displacement and moment-rotation behaviour of the connections were analysed, and initial stiffness, secant stiffness, and energy dissipation of the connections was compared. Pre-engineered connections had larger total energy dissipation when compared to the custom connections. The EVDR of pre-engineered connections generally increased throughout testing, while custom connections showed a decrease or plateau of

https://doi.org/10.52202/069179-0290

EVDR in the final primary cycles. As damage accumulated, all specimens experienced a degradation of secant stiffness throughout testing. By the final primary cycle of the cyclic testing protocol, all pre-engineered connections had the largest remaining secant stiffness, however, connection C4-MEG demonstrated a much gentler degradation of secant stiffness than the C5-MTCP connection, indicating more ductile behaviour. Similar to the monotonic testing, all connections maintained load carrying capacity throughout the testing protocol.

The data collected within this research is representative only of the five connection designs tested, therefore continued testing and investigation into the behaviour of a wider variety of beam-to-column connections is recommended. Additionally, increasing the cycle of maximum displacement to larger amplitudes would be recommended for future testing, so that the post-peak behaviour of connections could be observed. Examination of the post-peak behaviour of connections would allow for the calculation of connection ductility, as well as comparisons of post-peak degradation of strength and stiffness between different connection designs.

Additional research on numerical modelling methodologies for simulating these connections is necessary to expand the body of knowledge on the behaviour of glulam beam-to-column connections. Specifically, research on the development of material models that simulate crushing of timber in compression is necessary to perform predictive modelling of mass timber connections.

ACKNOWLEDGEMENT

This work was sponsored by the USDA Agricultural Research Service, grant no. 58-0204-6-002. Thank you to Holmes Structures, KPFF, and the Northwest Carpenters Union for donating time and expertise, and to Tyler DeBoodt for assistance during construction and testing.

REFERENCES

[1] American Society of Civil Engineers. *Minimum design loads and associated criteria for buildings and other structures.* ASCE/SEI 7-16. 2017. American Society of Civil Engineers. Reston, VA.

[2] American Wood Council (AWC). 2018. "National Design Specification for Wood Construction (ANSI/AWC NDS 2018)". *AWC.* Leesburg, VA.

[3] American Society for Testing and Materials (ASTM). 2021. "D7147-21:Specification for Testing and Establishing Allowable Loads of Joist Hangers". *ASTM International.* West Conshohocken, PA.

[4] Madland, H., Fischer, E.C., and Sinha. A. (2023). "Monotonic testing of glue laminated beam-to-column connections," *Journal of Structural Engineering*. 149(5).

[5] Madland, H., Fischer, E.C., and Sinha. A. (2023). "Cyclic testing of glue laminated beam-to-column connections," *Journal of Structural Engineering*. 149(4).

[6] Krawinkler H, Parisi F, Ibarra L, Ayoub A, Medina R. Development of a Testing Protocol for Woodframe Structures. 2001. *Consortium of Universities for Research in Earthquake Engineering.* Richmond, CA.

[7] Guo, J., & Shu, Z. (2019). "Theoretical Evaluation of Moment Resistance for Bolted Timber Connections," *MATEC Web of Conferences*, 303(201 9), 03003. https://doi.org/10.1051/matecconf/201930303003

[8] Jalilifar, E., Koliou, M., & Pang, W. (2021). "Experimental and Numerical Characterization of Monotonic and Cyclic Performance of Cross-Laminated Timber Dowel-Type Connections," *Journal of Structural Engineering*, 147(7), 1–20. https://doi.org/10.1061/(asce)st.1943-541x.0003059

[9] ANSI/APA. (2019). Standard for Performance-Rated Cross-Laminated Timber (ANSI/APA PRG 320-2019). *APA – The Engineered Wood Association*, Tacoma, WA.

[10] CEN (European Committee for Standardization). 2005b. *Timber structures – Test methods –Cyclic testing of joints made with mechanical fasteners*. EN12512:2001 including amendment A1:2005. Brussels, Belgium: CEN.

[11] Min-Juan, H., L. Hui-fen. (2015). *"*Comparison of glulam post-to-beam connections reinforced by two different dowel-type fasteners*." Construction and Building Materials.* 99(2015), 99-108. https://doi.org/10.1016/j.conbuildmat.2015.09.005.

[12] Li, Z., He, M., and Wang, K. 2018. "Hysteretic Performance of Self-Centering Glulam Beam-to-Column Connections". *Journal of Structural Engineering*, 144(5): 04018031. https://doi.org/10.1061/(ASCE)ST.1943-541X.0002012

[13] He, M., Luo, J., Tao, D., Li, Z., Sun, Y., & He, G. (2020). "Rotational behavior of bolted glulam beam-to-column connections with knee brace," *Engineering Structures*, 207(September 2019), 110251. https://doi.org/10.1016/j.engstruct.2020.110251

[14] Kharouf, N., McClure, G., & Smith, I. (2003). "Elasto-plastic modeling of wood bolted connections," *Computers and Structures*, 81(8–11), 747–754. https://doi.org/10.1016/S0045-7949(02)00482-0

[15] Leitner, E. (2011). *Three-Dimensional Modeling of Wood Moment Connections* (Issue May) [Pennsylvania State University]. file:///C:/Users/Tanner/Downloads/ejl195_-_MSc_Thesis.pdf

[16] Xu, B. H., Bouchaïr, A., & Racher, P. (2012). "Analytical study and finite element modelling of timber connections with glued-in rods in bending," *Construction and Building Materials,* 34, 337–345. https://doi.org/10.1016/j.conbuildmat.2012.02.087

[17] Hong, J.-P., & Barrett, D. (2010). "Three-Dimensional Finite-Element Modeling of Nailed Connections in Wood," *Journal of Structural*

Engineering, 136(6), 715–722. https://doi.org/10.1061/(asce)st.1943-541x.0000160

[18] Karagiannis, V., Málaga-Chuquitaype, C., & Elghazouli, A. Y. (2016). "Modified foundation modelling of dowel embedment in glulam connections," *Construction and Building Materials*, 102, 1168–1179. https://doi.org/10.1016/j.conbuildmat.2015.09.021

[19] Persson, J. (2011). *Numerical analysis of compression perpendicular to the grain in glulam beams with and without reinforcement* [Lund University]. http://www.byggmek.lth.se

[20] Chen, Z., Ni, C., Dagenais, C., & Kuan, S. (2020). "Wood ST : A Temperature-Dependent Plastic-Damage Constitutive Model Used for Numerical Simulation of Wood-Based Materials and Connections," *Journal of Structural Engineering*, 146(3), 1–14. https://doi.org/10.1061/(asce)st.1943-541x.0002524

https://doi.org/10.52202/069179-0290